

## CO4-1 Small Angle Neutron Scattering Study of Surfactant Micelle Structures by Utilizing KUR-SANS

K. Hara, T. Yanagino, S. Yoshioka,  
M. Sugiyama<sup>1</sup> and T. Fukunaga<sup>1</sup>

Faculty of Engineering, Kyushu University

<sup>1</sup>Research Reactor Institute, Kyoto University

### INTRODUCTION:

Hydrocolloids are composed of dispersoid and water; by the interactions between them, emerge the characteristic properties and structures. The authors have been interested in the nano-structures of the hydrocolloids; and in the previous study with utilizing KUR-SANS system, they successfully detected the alteration of the nano-scale micelle structure of sodium oleate (SO, Fig.1) with changing the ambient temperature [1], which also demonstrated the usability of the system in the investigations of the nanostructures of hydrocolloids. On the basis of the previous study, the authors have performed more extensive investigations by adding another surfactant, sodium decane sulfonate (SDS, Fig.1), as the specimen for the comparative SANS study.

### EXPERIMENTS:

Prepared were 1.0 wt% of SO and 3.0 wt% of SDS heavy-water solutions, which were sealed into respective quartz cells. After having been left intact for 24 hours at room temperature, observed were their small angle neutron scattering (SANS) profiles (Fig.2). Also, measured were the SANS profiles of the SO solutions with different concentrations (Fig.3). The SANS experiments were performed with a KUR-SANS spectrometer installed at Kyoto University Reactor, Kumatori, Osaka, Japan.

### RESULTS AND DISCUSSIONS:

Figure 2 shows the SANS profiles of 1.0 wt% of SO and 3.0 wt% of SDS heavy-water solutions, demonstrating the different features in their nano-structures. The relatively smaller structure in the SDS solution can come from their highly ionized hydrophilic heads and short-and-strait hydrophobic tails compared with SO composed of the weak-acid head and long-and-bent tails. From Fig.3, one can perceive a peak in the SANS profiles of SO with the concentrations above CMC, which indicates the micelle formation. The shape of the SANS profiles of SO in Figs.2 and 3 is characteristic and can be come from some complicated nano-structure. Detailed investigations are in preparation.

**REFERENCE:** [1] KURRI Prog. Rep. 2010, CO4-1, p. 210.

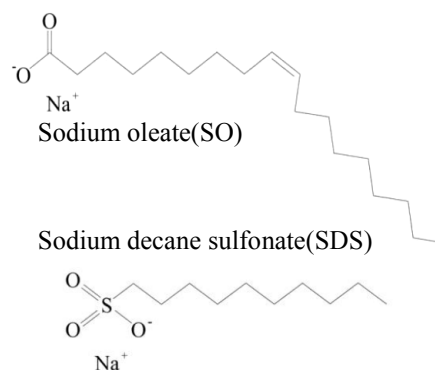


Fig.1 Chemical structures of the surfactants investigated in the present study.

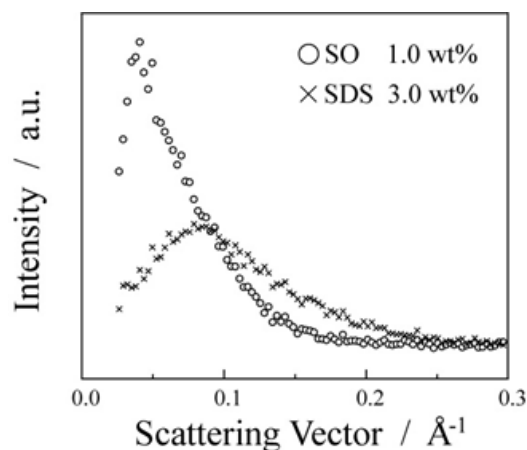


Fig.2 SANS profiles of SO and SDS measured by KUR-SANS system.

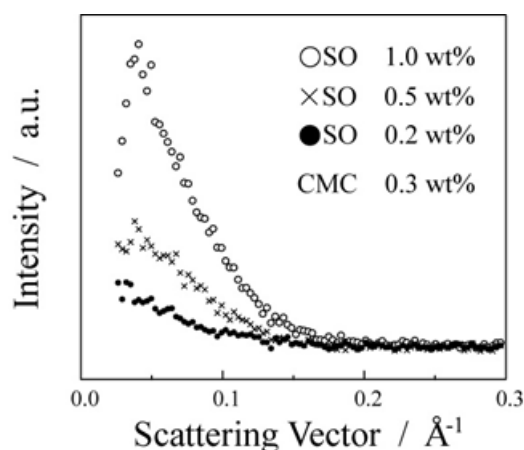


Fig.3 SANS profile change with SO-concentration measured by KUR-SANS system.

## CO4-2 Radiation-induced Luminescence for Applying to Retrospective Dosimetry

H. Fujita, Y. Nakano<sup>1</sup> and T. Saito<sup>1</sup>

Nuclear Fuel Cycle Engineering Laboratories, JAEA  
<sup>1</sup>Research Reactor Institute, Kyoto University

**INTRODUCTION:** It is well known that natural quartz exposed to ionizing radiation emits thermoluminescence (TL) such as ultra-violet TL (UVTL), blue TL (BTL) and red TL (RTL), and optically stimulated luminescence (OSL) [1]. The luminescence phenomena have been used for retrospective dosimetry (e.g. [2, 3]). However, the reason for the emission mechanisms of their luminescences except for BTL [4] from Japanese quartz has not yet been well explained. In this study, the emission mechanisms of UVTL, RTL and OSL were investigated in conjunction with various radiation-induced phenomena after annealing treatments of quartz samples, involving TL OSL and electron spin resonance (ESR) measurements.

**EXPERIMENTS:** Coarse quartz grains (150~250  $\mu\text{m}$ ) collected from surface soils in Japan were extracted by a general treatment of 6M hydrochloric acid (HCl) and 6M sodium hydroxide (NaOH) followed by concentrated hydrofluoric acid (HF) and sieving treatments. Further purification of the quartz grains was performed by hand selection for the sake of elimination of feldspar grains as low as possible under a microscope. The extracted quartz samples were annealed at 500 and 800  $^{\circ}\text{C}$  in an electric furnace. After the annealing treatment, the quartz samples were irradiated with  $^{60}\text{Co}$  source at room temperature at Kyoto University Research Reactor Institute (KURRI). After the  $\gamma$ -ray irradiation (the applied dose: 1 kGy), the sample was stored at room temperature for one day to eliminate afterglow effect in dark room. The ESR measurement was carried out using an ESR spectrometer (Jeol Ltd., JES-TE 200) at room temperature and  $-196^{\circ}\text{C}$ , respectively. Prior to the ESR measurements, the quartz samples were annealed for 1 min at 50  $^{\circ}\text{C}$  intervals ranging from 150 to 300  $^{\circ}\text{C}$  as preheat treatment. After the ESR measurements, all luminescence measurements were performed using a JREC automated TL/OSL-reader system installed with a small X-ray irradiator (Varian, VF-50J tube). All preparations were carried out under dim red light.

**RESULTS:** As shown in the previous report, the ESR signals of Ti-centers ( $[\text{TiO}_4/\text{H}^+]^0$ ,  $[\text{TiO}_4/\text{Li}^+]^0$  and  $[\text{TiO}_4/\text{Na}^+]^0$ ), Al-centers and RT-centers were detected in both quartz samples annealed at 500 and 800 $^{\circ}\text{C}$ . ESR

signal intensities of Ti-centers and Al-centers were decreased with the preheat temperatures but intensities of RT-centers were changed with the temperatures, randomly.

UVTL and RTL glowcurves, and OSL decay curves were measured using all kinds of quartz samples. The UVTL and the RTL intensities were integrated in whole region of heating temperature. The OSL signal intensity was estimated by integrating the counts in the first 1 s of the decay curve after subtracting the average background estimated from the data in the last 2 s of the OSL curve. Fig. 1 shows the changes of each luminescence intensity normalized to the intensity at 150  $^{\circ}\text{C}$ . The intensities of the UVTL and the RTL decreased with increasing preheat

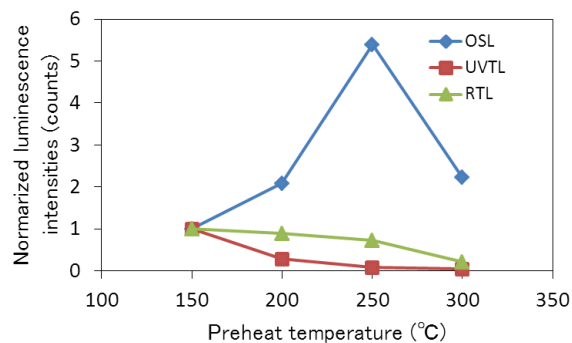


Fig. 1. Tendency of UVTL, RTL and OSL intensities with several preheat temperatures. Each luminescence intensity was normalized to the intensity at 150  $^{\circ}\text{C}$ .

temperatures. On the other hand, the intensities of OSL increased up to 250  $^{\circ}\text{C}$  and then decreased to 300  $^{\circ}\text{C}$ . The reason why the OSL intensity increased up to 250  $^{\circ}\text{C}$  is the re-trapping effect influenced by the preheat treatment.

In these results, the UVTL could be related to ESR signals of the Ti-centers but the other luminescences could not be related to ESR signals. Moreover, it is supposed that ESR signals of the Al-centers and the RT-centers have no relationship with TL and OSL.

Further work is necessary to identify luminescence mechanism using ESR measurement and annealing experiment.

### REFERENCES:

- [1] T. Yanmaguchi *et al.*, BUNSEKI KAGAKU **52** (2003) 787-793.
- [2] T. Hashimoto *et al.*, Radioisotopes **51** (2002) 10-18.
- [3] T. Hashimoto *et al.*, Radiat. Meas. **41** (2006) 1015-1019.
- [4] T. Hashimoto *et al.*, BUNSEKI KAGAKU **51** (2002) 527-532

T. Nakamoto, M. Yoshida, T. Ogitsu, Y. Makida,  
K. Yoshimura, S. Mihara, M. Sugano, H. Nishiguchi,  
M. Iio, Y. Kuno<sup>1</sup>, M. Aoki<sup>1</sup>, A. Sato<sup>1</sup>, T. Itahashi<sup>1</sup>, Q. Xu<sup>2</sup>,  
K. Sato<sup>2</sup>, Y. Kuriyama<sup>2</sup>, B. Qin<sup>2</sup>, Y. Mori<sup>2</sup> and  
T. Yoshiie<sup>2</sup>

J-PARC Center, KEK

<sup>1</sup>Department of Physics, Osaka University

<sup>2</sup>Research Reactor Institute, Kyoto University

**INTRODUCTION:** The superconducting magnets will be subjected to a high neutron fluence of  $10^{21}$  n/m<sup>2</sup> or higher in the operation life time in the high energy particle physics experiments with higher proton beam power, such as a high luminosity upgrade of the LHC at CERN and the muon source for the COMET experiment at J-PARC. Since electrical resistivity of a stabilizer at low temperature, which is very sensitive to neutron irradiation, is one of the important parameters for the quench protection of the magnet system. Measurement on aluminum stabilizer with additives of Y taken from the prototype superconducting cable as well as reference samples (5N pure aluminum and OFHC) was performed.

**EXPERIMENTS:** The irradiation test was carried out at a low temperature irradiation facility (LTL) at E-4 line of KUR. A sample with dimensions of 1 mm x 1 mm x 70 mm was cut from the aluminum stabilizer (RRR~350) of the superconductor manufactured by Hitachi Cable. The RRR of 5N aluminum and OFHC are 3000 and 300, respectively. The electric resistance was measured by a 4-wire method employing a Keithley 6221 current source and a Keithley 2182A voltmeter. Polyimide-coated wires were attached at both ends of the sample as current feeds and voltage sensing wires were attached with the interval of 45 mm on the sample by crimping with copper sleeves. A current of 100 mA was fed into the sample. The polarity was changed at a frequency of 10 Hz and the readouts were averaged over 100 cycles. The temperature was measured using a thermocouple of Au(Fe) and Chromel, since the Cernox sensor CX-1050-SD shows a temperature drift during neutron exposure maybe due to the irradiation damage. The thermocouple and the Cernox sensor and placed just behind the samples to measure the temperature of the helium gas.

**RESULTS:** Two aluminum stabilizer samples were irradiated in Nov. 2011. After cooling down to 10 K, the reactor was turned on to a power of 1 MW. The estimated fast neutron fluence in 52 hour operation is  $2.6 \times 10^{20}$  n/m<sup>2</sup>. Measured resistance and temperature changes during the irradiation are shown in Fig. 1. The temperature jumped from 10 K to 12 K at the beginning due to radiation from the reactor core. During exposure thermocouple indicates

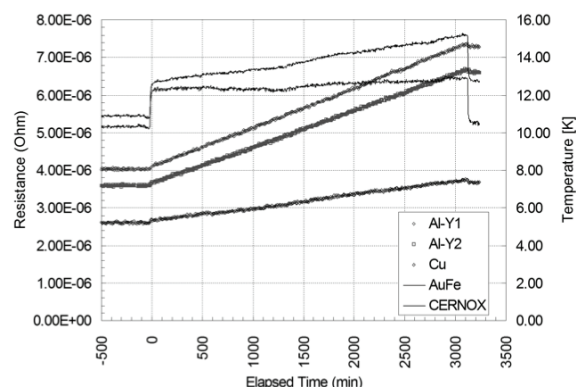


Fig. 1. Resistance and temperature of the aluminum stabilizer sample during irradiation.

stable temperature while the Cernox sensor readout drifts up to 15 K maybe due to irradiation damage. The sample resistance increased from  $4.0 \mu\Omega$  to  $7.3 \mu\Omega$  in 52 hours of exposure. Another sample changes from  $3.6 \mu\Omega$  to  $6.6 \mu\Omega$ . The resistance changes of the samples correspond to the induced resistivity of  $\rho_i = 0.067$ - $0.070$  n $\Omega$ m. The induced resistance seems to increase in proportion to the neutron fluence during exposure by a rate of  $d\rho_i = 0.027$  n $\Omega$ m per  $10^{20}$  n/m<sup>2</sup>. The 5N pure aluminum and OFHC samples are irradiated in Sep. 2011 at KUR. Due to troubles on data acquisition system, some data was lost and there exist noise in some part. The slope of resistance changes indicates  $d\rho_i = 0.027$  n $\Omega$ m per  $10^{20}$  n/m<sup>2</sup> for 5N pure aluminum, and  $d\rho_i = 0.008$  n $\Omega$ m per  $10^{20}$  n/m<sup>2</sup> for OFHC.

**SUMMARY AND PROSPECT:** A series of neutron irradiation tests at Kyoto Univ. Research Reactor has started, with the aim of R&D for radiation hard superconducting magnets. The electric resistivity in aluminum stabilizer for superconducting cable is investigated in this work. High strengthened aluminum stabilizer with yttrium doped were tested in 2011. Annealed 5N pure aluminum and OFHC were also irradiated as a reference data. Regardless of additives or transition by cold work, all the aluminum sample shows consistent degradation corresponding to the neutron-induced resistivity. The OFHC sample indicates less degradation by a factor of 3 than those of aluminum samples. While irradiation damage on the electrical conductivity of aluminum can recover by thermal cycling to the room temperature perfectly as observed in the previous work, irradiation damage in copper could remain after annealing at room temperature. Another irradiation test is planned to measure whether the degradation by iterative irradiation could be accumulated in copper.

S. Okuda, T. Kojima, S. Shimomura and T. Takahashi<sup>1</sup>

Radiation Research Center, Osaka Prefecture University  
<sup>1</sup>Research Reactor Institute, Kyoto University

**INTRODUCTION:** The coherent synchrotron and transition radiation (CTR) from electron bunches of a linear accelerator (linac) has continuous spectra in a submillimeter to millimeter wavelength range at extremely high peak-intensities. The coherent radiation (CR) light sources developed were applied to absorption spectroscopy [1-4] especially for matters with relatively strong light absorbance.

The absorption spectroscopy system using the CTR from the electron beams of the 45 MeV L-band electron linac was established at KURRI [5]. The CR has high-intensity pulsed electric field. This kind of light possibly excites matters in a short period. The change of the transmittance was observed in the measurements made by changing the light intensity [6]. However, the experimental configurations were not adequate for the study. In this work the previous absorption spectroscopy system has been slightly modified for such experiments.

**EXPERIMENTAL METHOD:** The new experimental configurations modified for the absorption spectroscopy investigating the effect of light intensity are schematically shown in Fig. 1. The output light from a light source chamber was focused at a light collimator 8 mm $\phi$  in diameter. The spectrum of light after passing through the sample was measured with a Martin-Puplett type interferometer and a liquid-He-cooled silicon bolometer. In the previous experimental configurations the sample was located on the light path between the interferometer and the detector [5]. The schematic diagram of the interferometer and the typical interferogram obtained by the measurement is shown in Fig. 2. The peak intensity of the pulsed light after the interferometer changes during the measurement.

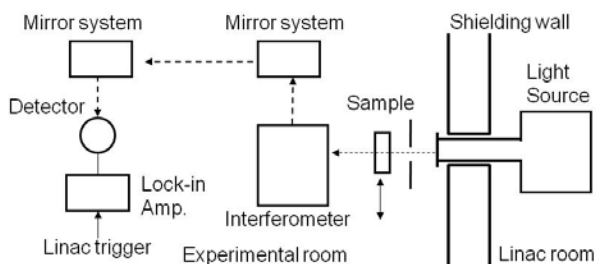


Fig. 1. Schematic diagram showing the new configurations for absorption spectroscopy using the CTR.

In this system the wavenumber resolution was 0.2  $\text{cm}^{-1}$ . It took about 5 minutes in a measurement. The spectrum was sufficiently stable during the measurements within  $\pm 2-3\%$  in a wavenumber range of 4-12  $\text{cm}^{-1}$ . The details

of the measurement are described in ref. 3.

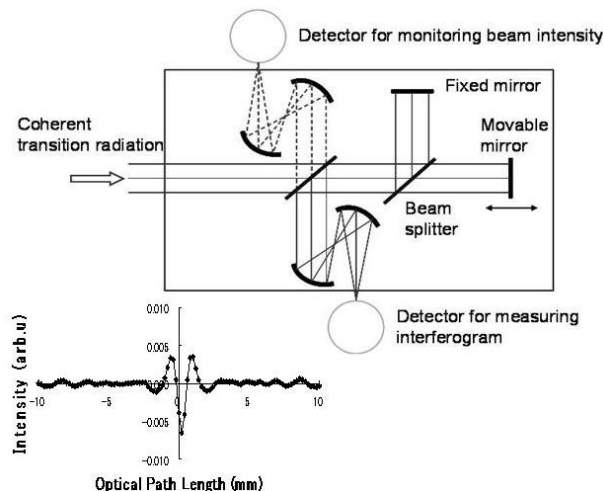


Fig. 2. Schematic diagram of the Martin-Puplett type interferometer and the typical interferogram obtained by the measurement.

**RESULTS AND DISCUSSION:** In the previous experimental configurations the wavenumber dependence of the transmittance of light was measured for various kinds of matters. For the sample of  $\text{SiO}_2$  nano particles the transmittance became higher by 20-30% at a light intensity two orders of magnitude higher than the ordinary one. These results seem to suggest some change in the conditions of the sample induced by the pulsed CTR. Measurements have been made under the new experimental configurations shown in Fig. 1. We are analyzing these new results obtained by the measurements.

In order to investigate the transient phenomena induced by the pulsed CR the pump-probe experimental system was established in Osaka Prefecture University.

#### REFERENCES:

- [1] T. Takahashi, T. Matsuyama, K. Kobayashi, Y. Fujita, Y. Shibata, K. Ishi and M. Ikezawa, *Rev. Sci. Instrum.* **69** (1998) 3770.
- [2] K. Yokoyama, Y. Miyauchi, S. Okuda, R. Kato and T. Takahashi, *Proc. 20th Int. Free-Electron Laser Conf. (Williamsburg, USA, 1998) II* 17-18.
- [3] S. Okuda, M. Nakamura, K. Yokoyama, R. Kato and T. Takahashi, *Nucl. Instrum. Meth.* **A445** (2000) 267.
- [4] S. Okuda, M. Takanaka, M. Nakamura, R. Kato, T. Takahashi, S. Nam, R. Taniguchi and T. Kojima, *Radiat. Phys. Chem.* **75** (2006) 903.
- [5] S. Okuda and T. Takahashi, *Infrared Phys. Technol.* **51** (2008) 410.
- [6] S. Okuda and T. Takahashi, *Proc. 35th Int. Conf. on Infrared, Millimeter and Terahertz Waves (2010, Rome, Italy)*, IEEE Xplore 10.1109/ICIMW.2010.5612474.



K. Konishi, Y. Shichibu, Y. Kamei, H. Ohashi<sup>1</sup> and Y. Kobayashi<sup>2</sup>

Faculty of Environmental Earth Science, Hokkaido University

<sup>1</sup>Faculty of Arts and Science, Kyushu University

<sup>2</sup>Research Reactor Institute, Kyoto University

**INTRODUCTION:** We have studied to prepare novel gold clusters because of their unique optical, electronic, and catalytic properties [1]. However, it is difficult to obtain such as electronic state of gold by X-ray single crystal structural analysis. It is important to obtain the bond information between gold cluster and ligand as cluster science and catalytic chemistry.

The aim of this study was to investigate the chemical state of gold in the ligand-coordinated gold clusters prepared.

**EXPERIMENTS:** Ligand-coordinated gold clusters ( $[\text{Au}_8(\text{dppp})_4](\text{NO}_3)_2$  and  $[\text{AuCl}_2(\text{dppp})_4](\text{NO}_3)_2$ , dppp = 1,3-bis(diphenylphosphino)propane) were prepared by the similar procedure reported before [1]. The chemical state of  $\text{Au}_N$  prepared was determined by  $^{197}\text{Au}$  Mössbauer spectroscopy (home-made equipment). The  $^{197}\text{Pt}$  isotope ( $T_{1/2} = 18.3$  h), a  $\gamma$ -ray source feeding the 77.3-keV Mössbauer transition of  $^{197}\text{Au}$ , was prepared by neutron irradiation of isotopically enriched  $^{196}\text{Pt}$  metal at the Kyoto University Reactor. The absorbers were particle specimens. The source and specimens were cooled with a helium refrigerator. The temperature of the specimens was in the range 8 – 15 K. The zero velocity point of the spectra was the peak point of pure bulk gold. The spectra for all the solid samples were fitted with a single Lorentzian function.

**RESULTS:** Figure 1 shows  $^{197}\text{Au}$  Mössbauer spectra of  $[\text{Au}_8(\text{dppp})_4](\text{NO}_3)_2$  and  $[\text{AuCl}_2(\text{dppp})_4](\text{NO}_3)_2$ , which superposing two components c1-c2 and c3-c4, respectively. Table 1 shows Mössbauer parameters for each component of these two cluster compounds. The spectrum of  $[\text{AuCl}_2(\text{dppp})_4](\text{NO}_3)_2$  was different from that of  $[\text{Au}_8(\text{dppp})_4](\text{NO}_3)_2$ , suggesting that Au-Cl bonds have a strong effect to Mössbauer parameters. The values of IS and QS in c1-c4 doublets are quite large, because the valence of gold is close to Au(I) and it has bonds to Cl or P. However, the resolutions of these peaks may or may

not be accurate because of shape of spectra because of shapes of these spectra. In the near future, the Mössbauer measurements of similar gold cluster compounds will help us to analyze details of assignment in these spectra.

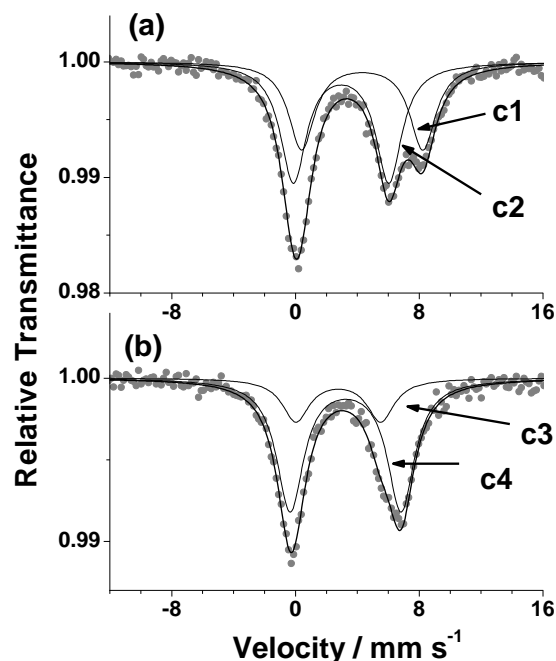


Fig. 1.  $^{197}\text{Au}$  Mössbauer spectra of  $[\text{Au}_8(\text{dppp})_4](\text{NO}_3)_2$  (a) and  $[\text{AuCl}_2(\text{dppp})_4](\text{NO}_3)_2$  (b).

**Table 1.** Mössbauer parameters for each component

Component	IS /mms <sup>-1</sup>	QS /mms <sup>-1</sup>	P /%	FWHM /mms <sup>-1</sup>
(a) c1	4.31	7.84	42.3	2.04
(a) c2	2.95	6.17	57.7	2.04
(b) c3	2.79	5.53	24.5	2.13
(b) c4	3.24	7.17	75.5	2.13

**REFERENCE:**

[1] Y. Shichibu and K. Konishi, *small*, **6**(2010)1216-1220.

T. Awano and T. Takahashi<sup>1</sup>

Department of Electronic Engineering, Tohoku Gakuin University

<sup>1</sup>Research Reactor Institute, Kyoto University

**INTRODUCTION:** Movement of ions is not in phase and frequent scattering by other mobile ions seems to decrease the ionic conductivity. If coherent excitation of ionic movement by coherent external electric field occurs, ionic conductivity seems to increase drastically. Coherent THz wave from LINAC of KURRI is so strong that the excitation effect is expected to be observed. We have measured millimeter wave absorption spectra of silver halides - silver phosphate glasses to investigate the existence of such a collective movement of conduction ion[1, 2]. In this study, it is tried to induce direct excitation of coherent ionic movement of conduction ion.

**EXPERIMENTS:** Thin and thick plates of  $\text{RbAg}_4\text{I}_5$  and  $\text{RbCu}_4\text{Cl}_3\text{I}_2$  between quartz windows were prepared from melt of these crystals. Transmittance spectra of coherent millimeter wave were measured by a Martin-Puplett type interferometer. Near field spectroscopic measurements were done by restricting field with light cone waveguide. Near electrode region was observed to study external field effect clearly. External electric field was applied by standard type function generator. Amplitude of the sinusoidal electric field was  $3.3V_{pp}$  and frequency was 1kHz. Gold thin wire was used as electrodes.

**RESULTS:** Figure 1 shows change of transmittance intensity of a thin plate of  $\text{RbAg}_4\text{I}_5$ . Transmittance spectrum in external field divided by that without external field is shown. Intensity decreased at  $6\text{ cm}^{-1}$  and  $10\text{ cm}^{-1}$ . Signal intensity was small around  $10\text{ cm}^{-1}$  because of strong absorption; therefore, only decrement around  $6\text{ cm}^{-1}$  is sure. This change recovered by removing the electric field. This means that the change is due to ionic conduction or secondary effect of the conduction, such as change of density of conduction ions. There still may be due to electrochemical reaction around electrodes.

Fig. 2 shows absorption spectra of  $\text{RbAg}_4\text{I}_5$  and  $\text{RbCu}_4\text{Cl}_3\text{I}_2$  crystal. No characteristic structure around  $6$  and  $8\text{ cm}^{-1}$ , which existed in glasses[1, 2], was observed in these crystals. This means that such absorption bands observed in glassy samples are related with random movement of conduction ions.

#### REFERENCES:

- [1] T. Awano and T. Takahashi, Journal of Physics: Conference Series **148** (2009) 012040.  
 [2] T. Awano and T. Takahashi, J. Phys. Soc. Jpn. **79** Suppl. A (2010) 118.

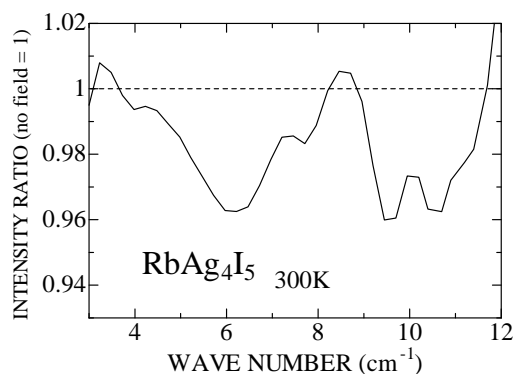


Fig. 1. Change of transmittance of  $\text{RbAg}_4\text{I}_5$  by applying external electric field. Measurement field was restricted around electrode by near field spectroscopic method.

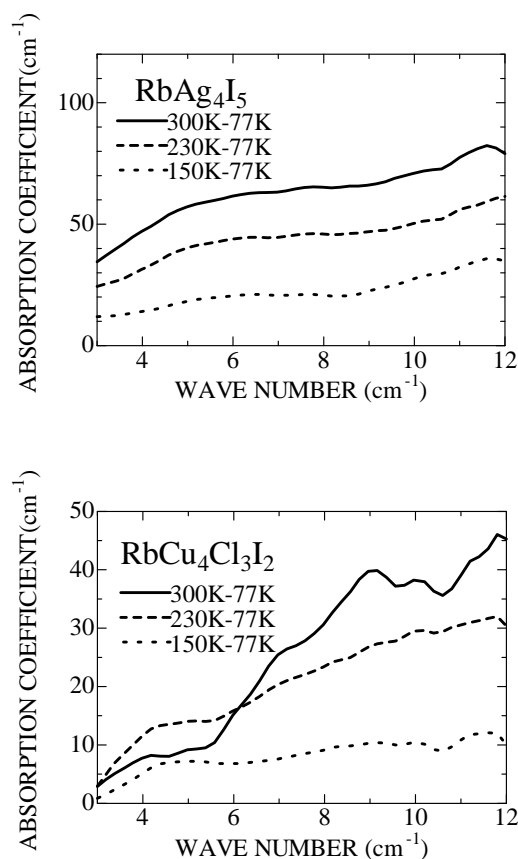


Fig. 2. Increment absorption spectra of  $\text{RbAg}_4\text{I}_5$  and  $\text{RbCu}_4\text{Cl}_3\text{I}_2$ . Absorption spectra at each temperature are subtracted by that at 77 K.

T. Takahashi, T. Iizuka<sup>1</sup> and S. Kimura<sup>2,1</sup>

*Research Reactor Institute, Kyoto University*

<sup>1</sup>*School of Physical Sciences, The Graduate University for Advanced Studies*

<sup>2</sup>*UVSOR Facility, Institute for Molecular Science*

**INTRODUCTION:** The basic properties of the technique of near-field THz-wave microscopy has been experimentally investigated by our group [1-3]. The technique is a characteristic application of coherent radiation emitted from a relativistic electron beam, and provides high spatial resolution below the diffraction limit. In the present report we have performed the one-dimensional imaging microscopy of a cancer tissue using a near-field aperture probe with coherent transition radiation (CTR) as the demonstration.

**EXPERIMENTAL PROCEDURES:** The experiment was performed at the coherent radiation beamline [4] at the 40-MeV L-band linac of the Research Reactor Institute, Kyoto University. The width of the macro pulse and the repetition rate of the electron beam were 47 ns and 46 Hz, respectively. The charge of a bunch was 1.2 nC. The THz-wave source was CTR emitted from an aluminum foil with a thickness of 15- $\mu\text{m}$ . The thickness of a cancer tissue was 50  $\mu\text{m}$  and was put between two sheets of Kapton film 25  $\mu\text{m}$  thick as shown in Fig. 1. The size of the aperture of the scanning probe was 775  $\mu\text{m}$ . The spectra of CTR were measured by a Martin - Puplett type interferometer at each scanning position of the sample.

**RESULTS:** The observed one-dimensional imaging spectra at the positions along the solid line in Fig. 1 were shown in Fig. 2. The dark color in this figure represents the large absorption by the sample. The absorption can be seen at around 11  $\text{cm}^{-1}$ . Similarly, the observed spectra at the position along the broken line in Fig. 1 were shown in Fig. 3. There seems to be the absorption at around 13  $\text{cm}^{-1}$ . The origin of this absorption is not clear at present.

**ACKNOWLEDGMENTS:** This work was partly supported by Quantum Beam Technology Program of MEXT, Japan.

#### REFERENCES:

- [1] T. Takahashi, *et al.*, KURRI-PR 2008 CO4-10.
- [2] T. Takahashi, *et al.*, KURRI-PR 2009 CO4-8.
- [3] T. Takahashi, *et al.*, KURRI-PR 2010 CO4-7.

[4] T. Takahashi, *et al.*, Rev. Sci. Instrum. **69** (1998) 3770.

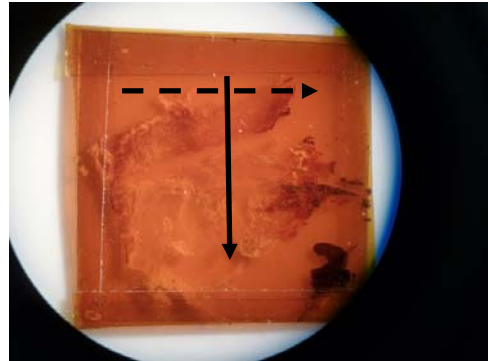


Fig.1. The photograph of the sample. The cancer tissue was put between two sheets of Kapton film.

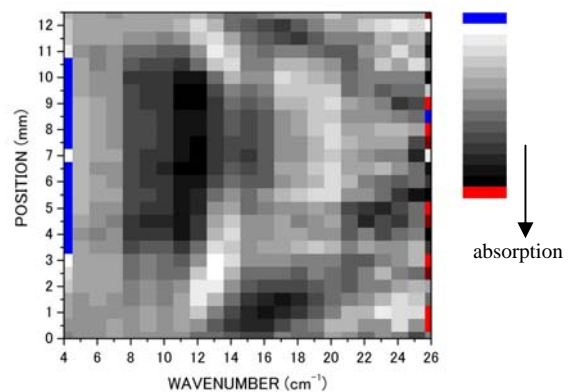


Fig.2. Observed spectra of transmitted THz wave at the positions along the solid line in Fig.1.

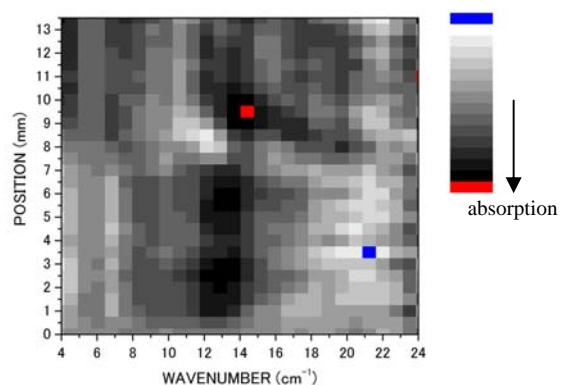


Fig.3. Observed spectra of transmitted THz wave at the positions along the broken line in Fig.1.

M. Ohnuma<sup>1</sup>, Y. Oba<sup>1,2</sup>, P.Kozikowsky<sup>1,3</sup> and M. Sugiyama<sup>2</sup>

<sup>1</sup>National Institute for Materials Science

<sup>2</sup>Research Reactor Institute, Kyoto University

<sup>3</sup>Warsaw University of Technology

**INTRODUCTION:** Precipitates in alloys often play an important role for modifying their properties in both structural and functional materials. Precipitation hardening is one of the key technology in structural materials and now widely used in the commercial products. Number density and average size of precipitates are dominant parameter for the level of increment in the mechanical properties. Though small-angle neutron scattering(SANS) is advantageous for obtaining such information in bulk form, shortage of machine time is serious problem for spread applications in steel industries. In addition, it is easy to prepare large samples that are stable at room temperature for the case of steel. Taking the above conditions into account, usage of small neutron source including both continuous and pulse is an urgent requirements for industrial applications. In this study, we applied KUR-SANS for the measurements of high-q SANS of steels for evaluating precipitates.

**EXPERIMENTS:** The steel with adding V to the S45C based compositions were measured using KUR-SANS. Wavelength used in the measurements is 0.26nm. Sample thickness is about 2 mm. Glassy carbon that is widely used as secondary standard for absolute unit was also measured. The obtained profiles were compared to the profiles measured using SANS-J-II installed in JRR-3. In this case, used wave length is 0.6nm.

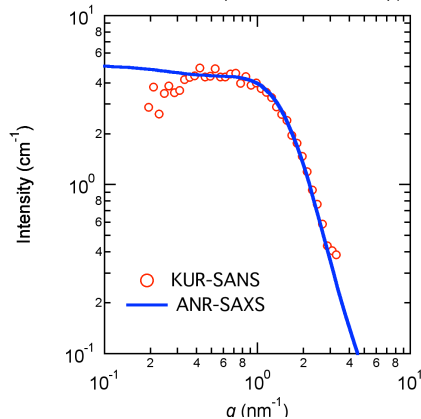


Fig. 1 SANS and SAXS profiles of glassy carbon measured by KUR-SANS and SAXS at ANL

**RESULTS:** Figure 1 shows a SANS profile of Glassy carbon measured for 4 hours at the running condition of 1MW of KUR. The profile shown in solid line is the one measured by small-angle X-ray scattering(SAXS) in Argonne National Labo(ANL), indicating that the data obtained in KUR is fine in the range of 0.3 to 3 nm<sup>-1</sup> which is the optimum q-range for characterizing nano-size precipitates. Figure 2 shows SANS profiles of the steel with Vanadium addition. The profiles were measured under the magnetic field of 0.5T to separate nuclear and magnetic scattering component. Although the q-range is same with the profiles of glassy carbon, profile shapes are not same with the one measured using SANS-J-II. Recent measurements using TAIKAN installed in J-PARC shows similar distortion of the profiles when the wave length below 0.4nm. Because the value correspond to the Bragg edge of 110 plane that is the maximum lattice plane in the bcc-Fe, the distortion of the profiles compare to the one measured using cold neutron with larger than Bragg cutoff wave length, can be attributed to the multiple diffraction.

Based on these results, we are now planning to use neutron with the wavelength larger than 0.4nm. Enlarging beam size from 5mm (present) to 10mm in diameter can cover the smaller neutron flux around this wavelength and make KUR-SANS useful tool in the steel research.

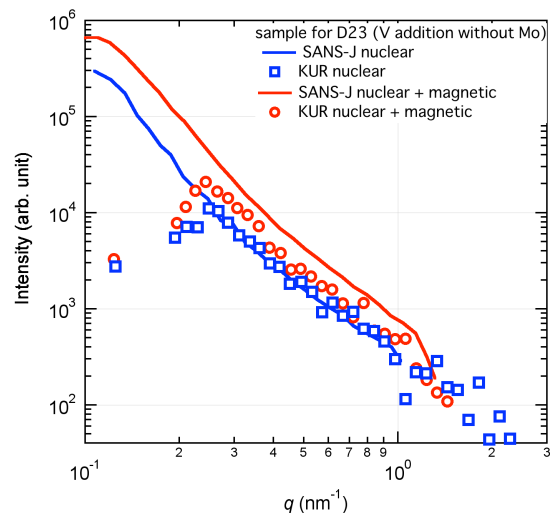


Fig. 2 SANS profiles of the steel with V measured by KUR-SANS and SANS-J-II at JRR-3



Y. Okaue, T. Yokoyama, H. Ohashi<sup>1</sup> and F. Yoshimura

Department of Chemistry, Faculty of Sciences, Kyushu University

<sup>1</sup>Faculty of Arts and Science, Kyushu University

**INTRODUCTION:** Trimethylsilylated silsesquioxane,  $Q_8M_8$  ( $[(CH_3)_3SiO]_8(SiO_{1.5})_8$ ), is a member of the cage-shaped oligosilsesquioxanes with cubic framework called double four-ring (D4R) structure as illustrated in Fig. 1. Upon  $^{60}Co$   $\gamma$ -ray irradiation at room temperature on  $Q_8M_8$ , stable hydrogen atom is encapsulated in D4R cage for the period of several years. The encapsulation and stabilization of hydrogen atom in D4R cage were confirmed by ESR spectroscopy. The hydrogen atom encapsulated in D4R cage of silsesquioxane interacts magnetically with paramagnetic oxygen molecules outside D4R cage to change ESR signal intensity and saturation behavior.[1] The purpose of this study was preliminary research for interactions between metal ions and encapsulated hydrogen atom within single molecule by introducing D4R cage structure of silsesquioxane to the ligand for metal ions. In this research, Schiff base ligand was used to form stable complexes with many metal ions easily.

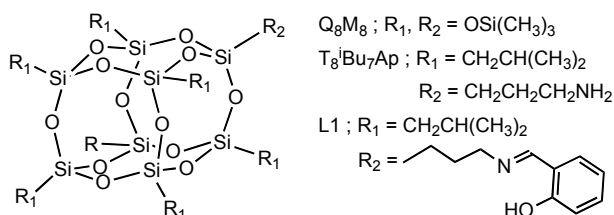


Fig. 1. D4R cage structure of silsesquioxanes.

**EXPERIMENTS:** New Schiff base ligand, L1, was synthesized by condensation of salicylaldehyde and  $T_8^tBu_7Ap$ , which is commercially available silsesquioxane with D4R cage structure as illustrated in Fig. 1. L1 and zinc(II) acetate dihydrate were stirred in methanol at 60 °C for 2 h. The resulting light yellow solution was concentrated under reduced pressure and cooled to room temperature. Zn(II) complex with L1 was produced as light yellow powder. In a similar manner, Cu(II) complex was also obtained as dark green powder. Characterizations were made by IR and  $^1H$  NMR spectroscopy and elemental analyses. Powder samples of L1 and the complexes with Zn(II) and Cu(II) were irradiated with  $\gamma$ -ray under air at room temperature in  $^{60}Co$   $\gamma$ -Ray Irradiation Facility at Kyoto University Research Reactor Institute. Irradiated samples were recrystallized from hexane. X-band ESR spectra for these recrystallized samples under air were measured on a JEOL JES-FA200 spectrometer at room temperature.

**RESULTS:** Ligand L1 was obtained as yellow powder. The maximum yield was ca. 40%. Light yellow Zn(II) complex was obtained as  $Zn(L1)_2$  in a 54% yield. Dark green Cu(II) complex was also obtained as  $Cu(L1)_2$  in a 77% yield.

ESR spectrum of the irradiated L1 was shown in Fig. 2 and ESR spectrum of the irradiated  $Zn(L1)_2$  was shown in Fig. 3. Characteristic two hyperfine lines separated with about 50 mT due to hydrogen atom nucleus ( $I=1/2$ ) were observed in these spectra. It was concluded that ligand L1 and the complex,  $Zn(L1)_2$ , can encapsulate hydrogen atom in the D4R cage of silsesquioxane unit. On the other hand, ESR spectrum of the irradiated  $Cu(L1)_2$  was typical spectral pattern due to Cu(II) species as shown in Fig. 4. Signals due to encapsulated hydrogen atom were also observed in enlarged spectrum, slightly.

### REFERENCE:

[1] R. Sasamori, Y. Okaue, T. Isobe and Y. Matsuda, *Science*, **265** (1994) 1691-1694.

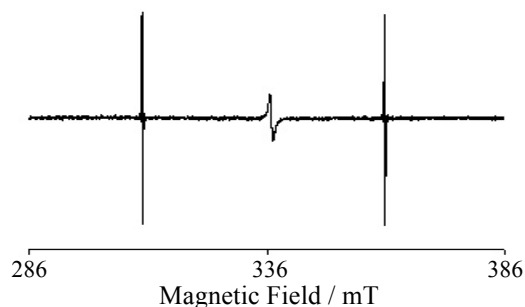


Fig. 2. ESR spectrum of irradiated L1.

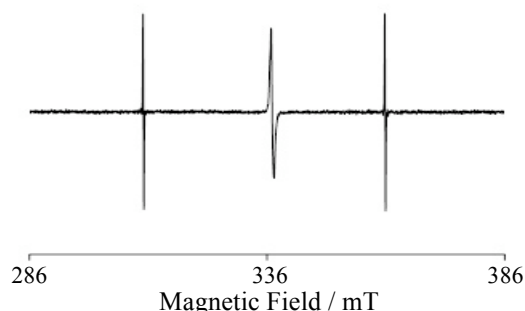


Fig. 3. ESR spectrum of irradiated  $Zn(L1)_2$ .

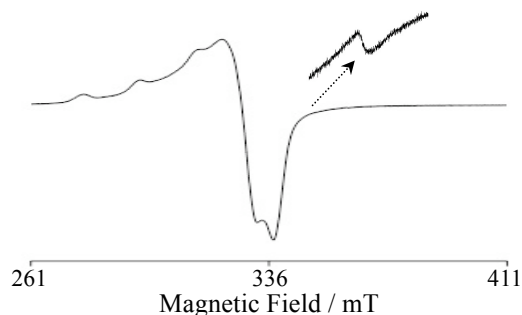


Fig. 4. ESR spectrum of irradiated  $Cu(L1)_2$ .

K. Munakata, K. Wada and T. Takeishi<sup>1</sup>

Department Faculty of Engineering and Resource Science, Akita University

<sup>1</sup>Graduate School of Engineering Science, Kyushu University

**INTRODUCTION:** The effect of titanium on the tritium release from  $\text{Li}_4\text{SiO}_4$  ceramic breeder material was investigated. Titanium was doped in  $\text{Li}_4\text{SiO}_4$  during the fabrication process so-called melt-spraying method. Tritium release curves were obtained in a series of experiments carried out using the out-of-pile temperature programmed desorption (TPD) technique. Tritium release curves obtained for solid breeders with different titanium composition were compared to examine the effect of catalyst metal on tritium release.

**EXPERIMENTS:** The titanium-doped  $\text{Li}_4\text{SiO}_4$  ceramic breeder materials were prepared and donated by Karlsruhe Institute of Technology (KIT). These ceramic breeders with catalytic metals encapsulated in a quartz tube were irradiated in Kyoto University Research Reactor (KUR) in the thermal neutron with the flux of  $5.5 \times 10^{14} \text{ cm}^{-2}\text{s}^{-1}$  in the He atmosphere.

Release curves of bred tritium from the breeder pebbles were obtained using the out-pile temperature programmed desorption techniques. The experimental apparatus is schematically shown by Figure 1. The volumes of ionization chambers are 66 cc and the time constant for replacement of the gas inside the chambers [volume] / [flow rate] is 40 seconds. The first ionization chamber was used to measure the total tritium concentration and the second chamber placed after a water bubbler was used to measure that of molecular form tritium in the purge gas, respectively.

Water vapor was introduced to the purge gas at the inlet of the ionization chamber when dry nitrogen gas or nitrogen with hydrogen gas was used as the purge gas to minimize the tritium memory effect according to the result obtained in the previous works.

**RESULTS:** Figure 2 shows comparison of experimental tritium release curves for the  $\text{Li}_4\text{SiO}_4$  samples irradiated for 30 minutes with neutron flux with  $5.5 \times 10^{14} \text{ cm}^{-2}\text{s}^{-1}$  [ $1/\text{cm}^2\text{s}$ ]. The sweep gases of 1,000 ppm  $\text{H}_2/\text{Ar}$  gas were used in the experiments. Comparison of Figs. 2(a) and (b) indicates that tritium is released at lower

relatively temperatures when titanium was doped to the  $\text{Li}_4\text{SiO}_4$  breeder material. With regard to the chemical form of tritium, almost all of the tritium was released as HTO for the both samples.

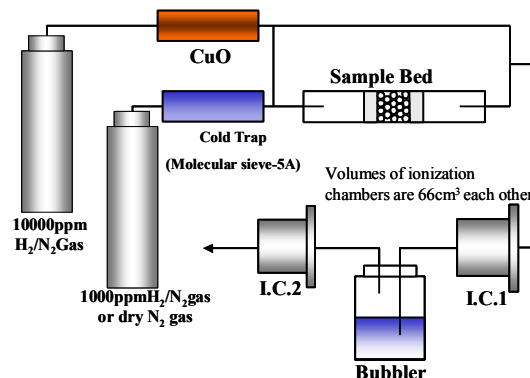


Fig.1. Schematic diagram of experimental apparatus.

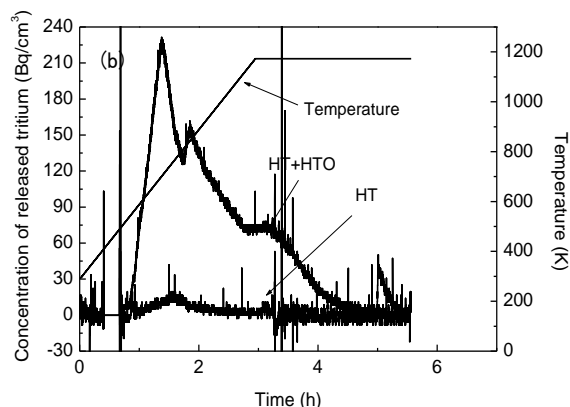
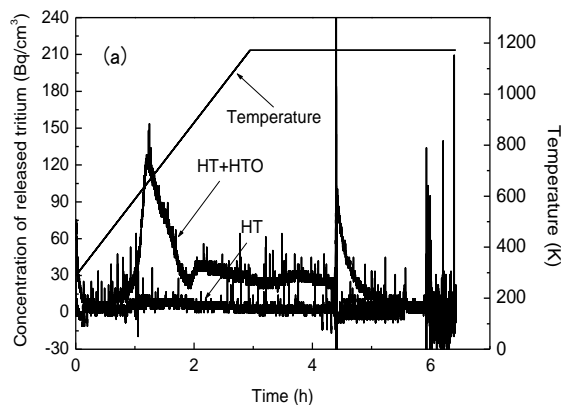


Fig. 2. Tritium release curves.

(a)  $\text{Li}_4\text{SiO}_4$  ceramic breeder material

(b)  $\text{Li}_4\text{SiO}_4$  ceramic breeder material

A. Nishimura and M. Sakamoto<sup>1</sup>

Department of Helical Plasma Research, National Institute for Fusion Science

<sup>1</sup>School of Physical Sciences, Sokendai

**INTRODUCTION:** The construction of a large scale plasma device, such as ITER or JT-60SA, is undergoing. These devices will perform Deuterium-Tritium (D-T) or D-D reaction and generate a lot of fusion neutrons with 14 MeV. Some fusion neutrons will penetrate the blankets or stream out of the ports and reach the superconducting magnets. The superconducting magnets consist of the stabilizer such as high purity copper and aluminum, the electric insulation materials, the superconducting materials and the structural materials. The stabilizer will carry the running current when the superconducting material becomes normal by temperature rise. The electric resistance of the high purity copper and the aluminum changes after the neutron irradiation ( $> 0.1$  MeV) of order of  $10^{19}$  to  $10^{20}$   $n/m^2$ . The insulation materials are the epoxy resin basis. To improve the neutron and gamma ray irradiation resistance, the cyanate ester blended with the epoxy has been developed for the ITER superconducting magnets. In case of ITER, the neutron fluence of  $1.0 \times 10^{22}$   $n/m^2$  is a design value. Some typical results will be presented later. Regarding the superconducting material, the changes in the critical current and the critical temperature of superconducting strands by the neutron irradiation have been investigated and the study on the critical magnetic field started. The recent results will be shown below. The irradiation effect on the structural material such as Type 316L stainless steel has been investigated and the change in the mechanical properties has been found in the range of the neutron fluence of order of  $10^{24}$  to  $10^{25}$   $n/m^2$ .

**EXPERIMENTS:** The insulation sample (a kind of GFRP) was hand-made by laminating a glass fiber cloth and a polyimide film followed by impregnation of the blended resin. The size of the sample was  $10 \text{ mm}^W \times 15 \text{ mm}^L \times 2.5 \text{ mm}^t$ . After the neutron irradiation at JRR-3, JAEA, or the gamma ray irradiation with  $^{60}\text{Co}$ , the 3-point bending spanning 12.5 mm was carried out at 77 K and the interlaminar shear strength (ILSS) was evaluated. As for the superconducting strands, the 14 MeV neutron irradiation was carried out at FNS, JAEA, and the superconducting properties were measured using 28 T superconducting magnet at HFLSM, Tohoku University.

**RESULTS:** The ILSS results are shown in Fig. 1. CTD and MCE indicate the Cyanate ester and EP indicates the epoxy, and the blend ratio was varied. It should be noted that the lower fraction of the cyanate ester brings the

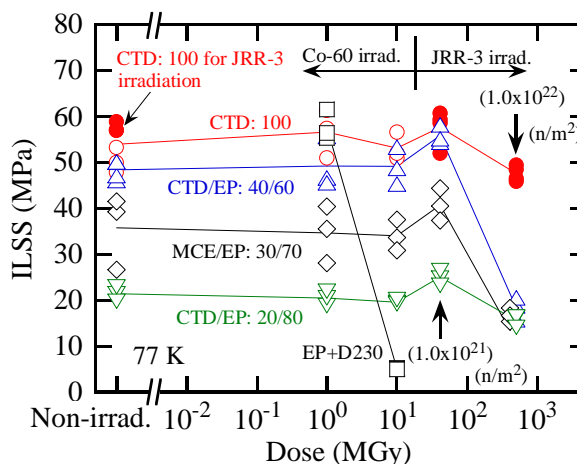


Fig. 1 Relation between ILSS at 77 K and dose.

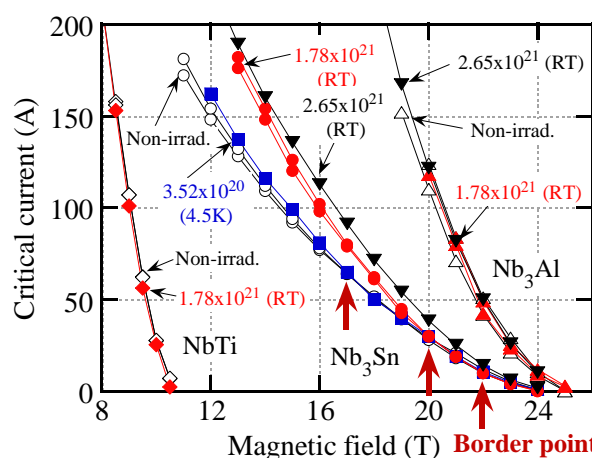


Fig. 2 Change in critical current of NbTi, Nb<sub>3</sub>Sn and Nb<sub>3</sub>Al strands.

lower ILSS and the ILSS does not drop at the dose of about 50 MGy at least. However, when the dose increased to about 500 MGy, the ILSS except for the case of 100 % cyanate ester dropped significantly. In a practical point of view, the pot life is important to handle the resin. The results of the critical current measurements of NbTi, Nb<sub>3</sub>Sn and Nb<sub>3</sub>Al strands are shown in Fig. 2. The maximum fluence achieved is  $2.65 \times 10^{21}$   $n/m^2$ . In case of the Nb<sub>3</sub>Sn, the critical current improved by the neutron irradiation, as far as the test was carried out, especially in the lower field. Since the magnetization diagram (M-H curve) was expanded by  $1.0 \times 10^{22}$   $n/m^2$  irradiation, the critical current would increase more. However,  $1.0 \times 10^{24}$   $n/m^2$  irradiation made the M-H hysteresis shrink and the strand would not become superconducting at 4.2 K. The critical temperature of  $2.65 \times 10^{21}$   $n/m^2$  irradiated sample decreased by 0.2 K. These changes would be caused by the knock-on effect of the fast neutron.

## CO4-12 Complex Structure of Ions Coordinated with Hydrophilic Polymer. 12: Stain Growth on Composite under DC Field

A. Kawaguchi, Y. Gotoh<sup>1</sup> and Y. Morimoto

KURRI

<sup>1</sup>Faculty of Text. Sci. and Tech., Shinshu Univ.

**INTRODUCTION:** We have reported in situ composite structure through "secondary doping" by diffusion of metallic ions into the iodinated hydrophilic polymers. Polyiodide ions,  $I_n^-$  ( $n = 3, 5, \dots$ ), which have been doped into the polymers previously, enhances following diffusion of other molecules or ions at room temperature.[1,2] As the easiest case for diffusing operation of metallic ion, we have achieved spontaneous diffusion of silver ion ( $Ag^+$ ) from  $AgNO_3(aq)$  into "iodinated polyamide-6 (PA6, Nylon<sup>TM</sup>-6)". This process can develop precipitation of inorganic salt at inner space of polymeric matrix and consequently provides hybrid composite for unlimited shape or size without plasticizing matrix.[3,4] On the other hand, such spontaneous diffusion can not always advance easily for some other metallic cations; there is dependence on ionic species for both complex structure and diffusion efficiency.[5]

However, in spite of such dependence, ionic diffusion and conductivity in iodinated polymers certainly suggest a view as electrolyte, and we can expect possibility of enforced diffusion of ions driven by applied voltage. Or, experimental results with SANS data suggest that swelling can induce resolution of silver iodide (AgI) salt grain as fillers which precipitated in the composite even though AgI is hardly soluble in water.[6] As the first step, behavior for ionic conduction was investigated with " $Ag^+/I_n^-/PA6$  (hybrid) composite" under applying electrical field.

**EXPERIMENTS:** Commercial filmy products "Rayfan #1401" in thickness of 0.1mm (Toray Film co.ltd.), was used as non-doped PA6. After annealing at 210 °C in vacuum, a piece of PA6 film was immersed into  $KI-I_2(aq)/0.8N$  (iodine-doping). Next, aged in vacuum at R.T., the iodine-doped PA6 film was immersed into  $AgNO_3(aq)/0.1M$  (secondary doping of  $Ag^+$ ). After dried in vacuum again, this filmy sample was clipped with platinum plates as conduction probes; both an anode and a cathode were Pt. Applying DC10V, the sample was held in a humid vessel keeping RH 60-85% at R.T.

**RESULTS AND DISCUSSION:** After secondary doping of  $Ag^+$ , the samples showed "light yellow" color similar as AgI salt ("stage II", Fig.1a)[7] In dried stage, the sample did not indicate explicit conduction current by DC10V ( $I < 10^{-8}A$ ), but conduction was observed after the sample held with the Pt probes was transferred in the humid environment; monitored current was fluctuated as  $10^{-6}A$  range, but quantitative discussion has not been achieved since estimation of film thickness and

uniformity of the sample were not confirmed.

On the other hand, appearance of the sample varied with applying voltage; "black stain" like expanding branches grew from the cathode (negative probe) to the anode (positive probe). (Fig.1b-d) However, expansion of the stain did not show any effects for conduction; while current was observed after transferring in humid environment, it was hardly changed in each stage of growth of "black stain", before it appeared on the edge of the cathode or after it reached the anode. After experiments, surface area behind the cathode seemed to stand still as ordinary sample while region behind the anode partially turned to black. (Fig.1e)

It is regarded that "black stain" growing from the cathode to the anode was not reduced  $Ag(0)$  since it did not contribute to conduction; it may be  $Ag_2O$  or insulative compounds. Nevertheless, DC conduction and ionic transfer (behind the anode) were induced by support of swelling process at room temperature. On the other hand, AgI which is main components of precipitates as filler in the hybrid composite is known as inorganic salt hardly soluble to water and indicating ionic conduction. Present results complementary to previous SANS experiments indicate that iodinated polymer can be regarded as "pseudo solvents" and that ionic diffusion can advance through polymeric matrix at room temperature.

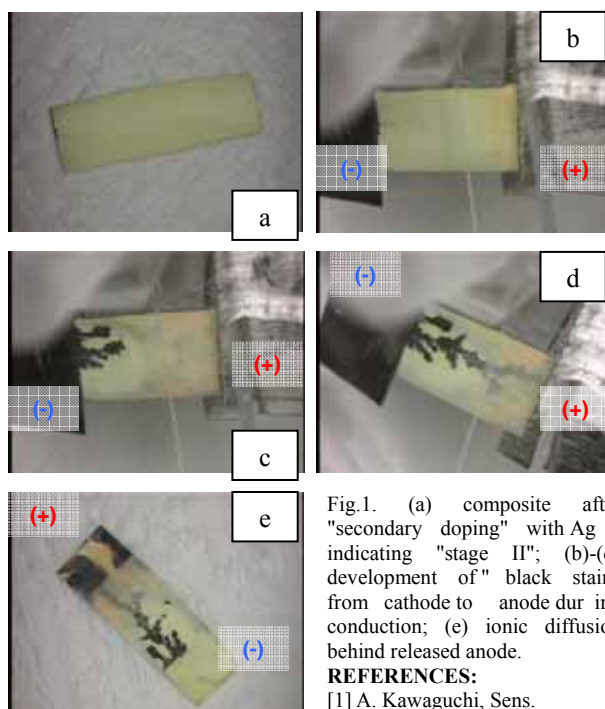


Fig.1. (a) composite after "secondary doping" with  $Ag^+$ , indicating "stage II"; (b)-(d) development of "black stain" from cathode to anode during conduction; (e) ionic diffusion behind released anode.

### REFERENCES:

- [1] A. Kawaguchi, Sens. Actuators B, **73** (2001) 174-178.  
 [2] Y. Gotoh, *et al.*, Polym. Prep. Jpn., **51** (2002), 2259-2259.  
 [3] A. Kawaguchi, *et al.*, *ibid.*, **53** (2004), 3372-3372.  
 [4] A. Kawaguchi, *et al.*, *ibid.*, **56** (2007), 5471-5472.  
 [5] A. Kawaguchi, Sens. Actuators B, **63** (2000) 10-17.  
 [6] A. Kawaguchi, *et al.*, KURRI Prog.Rep., 2002 (2003), 20-20.  
 [7] A. Kawaguchi, *et al.*, Polym. Prep. Jpn., **53** (2004), 3737-3738



T. Takahashi

Research Reactor Institute, Kyoto University

**INTRODUCTION:** For the spectroscopic purpose, various types of coherent radiation emitted from a relativistic electron beam have attracted a considerable attention as a new and powerful light source in the THz-wave region. Coherent transition radiation (CTR) is one of such a light source. Whereas synchrotron radiation has linear polarization along an electron orbit, the electric vector of transition radiation (TR) emitted from a metallic screen is axially symmetric with respect to the trajectory of an electron beam. Therefore, CTR is usually utilized as a non-polarized light source in the spectroscopic application. However, circularly polarized light has been useful in the circular dichroism spectroscopy. I have proposed a new technique of generation of circularly polarized THz-wave radiation with wire-grid radiators. [1]. In this report the property of polarization with some radiators has been experimentally investigated.

**EXPERIMENTAL PROCEDURES:** The experiment was performed at the coherent radiation beamline [2] at the 40-MeV L-band linac of the Research Reactor Institute, Kyoto University. The width of the macro pulse and the repetition rate of the electron beam were 47 ns and 46 Hz, respectively. The average current of the electron beam was 1.8  $\mu$ A. The schematic layout of the experiment is shown in Fig. 1. As a forward radiator (FR in Fig. 1) of forward CTR a wire grid 10  $\mu$ m thick with 25mm spacing was used. A flat aluminum foil 15  $\mu$ m thick and a wire grid were prepared as backward radiators. The direction of the wire grid was vertical. The CTR was detected by a liquid-helium-cooled Si bolometer. In order to measure the polarization a wire-grid polarizer was used in front of the detector.

**RESULTS:** The intensity variation as a function of the azimuth angle of the polarization was observed by rotating the wire-grid polarizer. The observed intensity with the aluminum-foil backward radiator is shown by the open squares in Fig. 2. Zero degree corresponds to the vertical component of radiation. The polarization of observed radiation was horizontal. On the other hand, the polarization of radiation from the wire-grid backward radiator (open circles in Fig. 2) was perpendicular. The

superposition of forward and backward radiation was observed in this configuration. Therefore, it was clearly represented by these results that the horizontal polarized radiation was emitted by the wire-grid forward radiator and the backward radiation from the wire-grid backward radiator had a vertical polarization. The polarization of backward radiation from an aluminum foil was radially. This conclusion will lead to the development of the high-resolution time-resolved circular dichroism spectroscopy in the THz-wave region.

### REFERENCES:

- [1] T. Takahashi, *et al.*, KURRI-PR 2008 CO4-6.
- [2] T. Takahashi *et al.*, *Rev. Sci. Instrum.* **69** (1998) 3770.

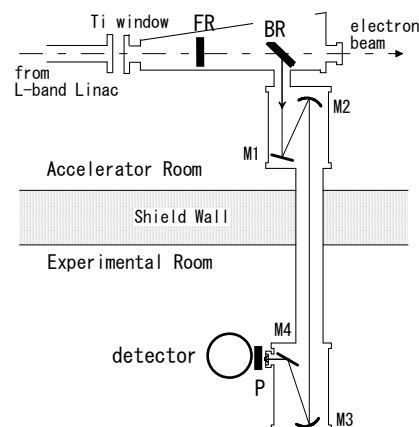


Fig.1. The arrangement of the experiment. Keys are: (FR) a forward radiator, (BR) a backward radiator, (M1, M4) flat mirrors, (M2, M3) spherical mirrors, (P) a polarizer.

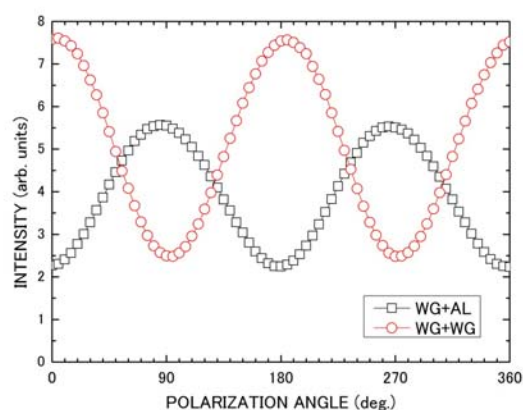


Fig.2. Intensity variation of CTR with a wire-grid (open squares) and an aluminum foil (open circles) as a backward radiator. The intensity of open circles was multiplied by ten.



K. Okuno, Y. Oya, M. Kobayashi, J. Osuo, M. Suzuki, A. Hamada, K. Matsuoka, K. Kawasaki, T. Fujishima, Y. Miyahara, H. Uchimura, T. Taguchi, K. Toda, R. Miura, T. Fujii<sup>1</sup>, and H. Yamana<sup>1</sup>

Radioscience Research Laboratory, Faculty of Science,  
Shizuoka University

<sup>1</sup>Research Reactor Institute, Kyoto University

**INTRODUCTION:** For the development of D-T fusion reactors, it is important to establish an effective fuel recycling system and a comprehensive model of tritium migration processes in solid tritium breeding materials. In the test blanket module for ITER, lithium titanate ( $\text{Li}_2\text{TiO}_3$ ) is a candidate as tritium breeding materials. Recently, the use of  $\text{Li}_{2+x}\text{TiO}_3$  ( $x=0.2, 0.4$ ), which is the lithium-enriched  $\text{Li}_2\text{TiO}_3$ , is proposed to improve the tritium breeding ratio [1,2].

In this study, thermal neutron irradiation was carried out to evaluate tritium diffusivities in  $\text{Li}_{2+x}\text{TiO}_3$  ( $x=0, 0.2, 0.4$ ). Therefore, out-of-pile tritium release experiments under isochronal and isothermal heating were performed. Comparing to Arrhenius parameters of tritium diffusion in these materials, the effects of excess lithium on tritium release were also discussed.

**EXPERIMENTAL:** Powders of  $\text{Li}_{2+x}\text{TiO}_3$  purchased from Kaken Co. were used as samples. The average grain diameters of  $\text{Li}_{2.0}\text{TiO}_3$ ,  $\text{Li}_{2.2}\text{TiO}_3$  and  $\text{Li}_{2.4}\text{TiO}_3$  measured by SEM were 3.0, 1.0 and 1.0  $\mu\text{m}$ , respectively. The samples were introduced into quartz tubes individually and annealed at 1173 K. Thermal neutron irradiations were conducted at Pneumatic tube 2 (Pn-2) of Research Reactor Institute, Kyoto University (KURRI). The thermal neutron flux was  $5.5 \times 10^{12} \text{ n cm}^{-2} \text{ s}^{-1}$ . The thermal neutron irradiation was carried out for 10 min, corresponding to the thermal neutron fluence of  $3.3 \times 10^{15} \text{ n cm}^{-2}$ . Out-of-pile tritium release experiments were performed in tritium-TDS (Thermal Desorption Spectroscopy) system at Shizuoka University. TDS spectra obtained in isochronal annealing experiments were simulated by using above-mentioned Arrhenius parameters obtained by isothermal annealing experiments to confirm the adequacy of this work.

**RESULTS&DISCUSSION:** Figure shows the tritium TDS spectra for  $\text{Li}_{2+x}\text{TiO}_3$ . Major tritium release stages

were located around 600 K for all  $\text{Li}_{2+x}\text{TiO}_3$  samples. In addition, tritium release around 450 K was clearly found for  $\text{Li}_{2.4}\text{TiO}_3$ . These tritium release stages around 450 and 600 K were named as Peaks 1 and 2, respectively. The release rate of Peak 1 at lower temperature side was increased as the amount of excess lithium increased, which was attributed to the release of tritium trapped in  $\text{Li}_4\text{TiO}_4$  structure. Peak 2 was considered to a release of tritium trapped by irradiation defects in  $\text{Li}_2\text{TiO}_3$ .

Isothermal annealing experiments indicated that tritium releases were controlled by diffusion process. The diffusion coefficient for  $\text{Li}_{2.0}\text{TiO}_3$  was one order of magnitude as large as those for  $\text{Li}_{2.2}\text{TiO}_3$  and  $\text{Li}_{2.4}\text{TiO}_3$ , although activation energies for these ceramics were almost the same to be 0.59 eV. These results showed that activation energy was determined by the diffusion process of tritium in  $\text{Li}_2\text{TiO}_3$  structure and excess lithium would reduce the diffusion coefficients and activation energies, which was quite low compared to previous data [3], indicating that it would be caused by the existence of  $\text{Li}_4\text{TiO}_4$  structure.

The simulation of TDS spectra using Arrhenius parameters obtained by isothermal annealing experiments was compared with the present experimental results. It was found that the rate limiting process of tritium release under He atmosphere was the diffusion process. However, surface reactions are also quite important for actual fusion reactor and further studies using different purge gas are required for the comprehensive understanding of tritium migration in tritium breeding materials.

#### REFERENCES:

- [1] T. Hoshino et al., J. Nucl. Mater., 386 (2009) 1098.
- [2] J. Osuo et al., Fusion Eng. Des, 86 (2011) 2362
- [3] T. Kinjo et al., Fusion Eng. Des. 83 (2008) 580.

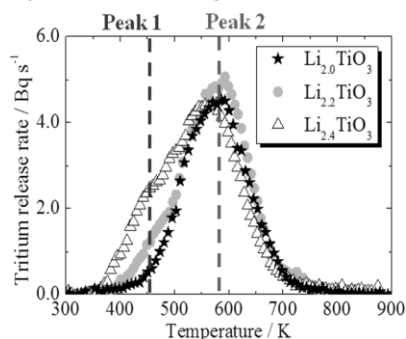


Fig. Tritium-TDS spectra for  $\text{Li}_{2+x}\text{TiO}_3$  with heating rate of 0.5 K/min